Int. J. Heat Mass Transfer. Vol. 22, pp. 1557–1565

0017–9310/79/1101–1557 $02.00/0

THE CALCULATION OF FREE TURBULENT SHEAR FLOWS WITH STRONG DENSITY FLUCTUATIONS

W. KOLLMANN and D. VANDROMME
von Karman Institute for Fluid Dynamics, B-1640 Rhode Saint Genèse, Belgium

(*Received* 27 *December* 1978)

Abstract—The turbulent mixing of two gases with highly different molecular masses in a plane shear layer is considered. A calculation model incorporating modelled transport equations for the partial density fluctuations is developed and the numerical results are compared with measurements showing good agreement.

NOMENCLATURE

c_p
$c_{\varepsilon_1}, c_{\varepsilon_2}, c_{\varepsilon_3}$
c_{Q_1}, c_{Q_2} } constants in turbulence model;
c_i, mass fraction;
D, divergence of velocity;
$\mathscr{D}_i$, molecular diffusivity;
$f_{x\beta}$, stress tensor;
J_{ix}, diffusive mass flux of component i in direction α;
k, kinetic energy of turbulence;
N, number of species;
O, order of magnitude;
Q_{ij}, correlation of partial densities;
p, pressure;
Re, Reynolds number;
R_i, gas constant of component i;
u,v, velocity components;
v_x, velocity vector;
t, time;
T, temperature;
x,y,x_α, Cartesian coordinates.

Greek symbols

α, pressure gradient parameter;
δ_1, characteristic thickness;
$\delta_{\alpha\beta}$, Kronecker-symbol;
ϕ
ψ } flow variables;
ρ, density;
σ, Prandtl/Schmidt number;
μ, dynamic viscosity;
ε, dissipation rate of k.

Superscripts

~, Favre-average;
″, Favre-fluctuation;
—, unweighted average.

Subscripts

A,B, components in binary mixture;
i, species;
0, reference value;
t, turbulent;
α,β,γ, Cartesian coordinates;
ϕ, flow variable.

1. INTRODUCTION

THE TURBULENT mixing of two gases with different molecular mass in a free shear flow is of interest for the basic understanding of the turbulent mixing process as well as for technical applications. The plane mixing layer at subsonic speeds is considered where helium and nitrogen mix turbulently. The difference in molecular masses produces strong density fluctuations at a level which is comparable to the density fluctuations that can be expected in turbulent combustion processes such as turbulent H_2–air diffusion flames. A calculation model based on the k–ε model [10] is developed incorporating transport equations for partial density correlations. The calculations are compared with measurements by Rebollo [1] and show good agreement. It turns out that the turbulent transport of mass in this particular flow has some interesting peculiarities, namely a surprisingly small turbulent Schmidt number and as a consequence, an overshoot of the dynamic pressure on the high velocity–low density side. Both features are correctly represented by the calculation model.

2. FLOW CONFIGURATION

The type of turbulent flows considered are plane free shear flows in the form of mixing layer or jet. Two gases with different molecular masses, which have at the same pressure and temperature different densities, enter the flow regime separated by a thin wall as parallel streams with different velocities (see Fig. 1). The two components mix in the developing shear layer. Due to the different densities of the entering streams, the turbulent mixing in the shear layer will show a fluctuating total density. A selected set of experimental data for this kind of turbulent shear flow with density fluctuations was provided by Rebollo [1]. He considered the plane mixing layer in which the upper stream consists of helium and the

lower stream of nitrogen. The velocities and densities on the upper and lower boundaries under a pressure $p = 4$ atm. are:

$$\text{helium} \quad \rho_2 = 0.641\,\text{kg m}^{-3}, \quad u_2 = 10.9\,\text{m s}^{-1}$$

$$\text{nitrogen} \quad \rho_1 = 4.49\,\text{kg m}^{-3}, \quad u_1 = 4.18\,\text{m s}^{-1}.$$

The free stream Reynolds numbers per unit length are then $Re_2 = 3600\,\text{cm}^{-1}$ (helium) and $Re_1 = 12000\,\text{cm}^{-1}$ (nitrogen) and the flow satisfies the equilibrium condition

$$\rho_1 u_1^2 = \rho_2 u_2^2. \tag{1}$$

stream values and laminar boundary layer profiles at the upper and lower side of the splitter plate. The turbulence quantities k and ε are given as small values such that a turbulent viscosity of the order of the molecular one is produced. The mean concentration is a step function at the end of the splitter plate and the density correlations are set to zero. The conditions at the upper and lower boundary of the flow regime are of Dirichlet type for mean values and of Neumann type for second order moments.

Among the numerous experimental results concerning free shear flows (see [2], and [3, 4]) only few are concerned with longitudinal pressure gradient or variable density. Brown and Roshko [5] studied the

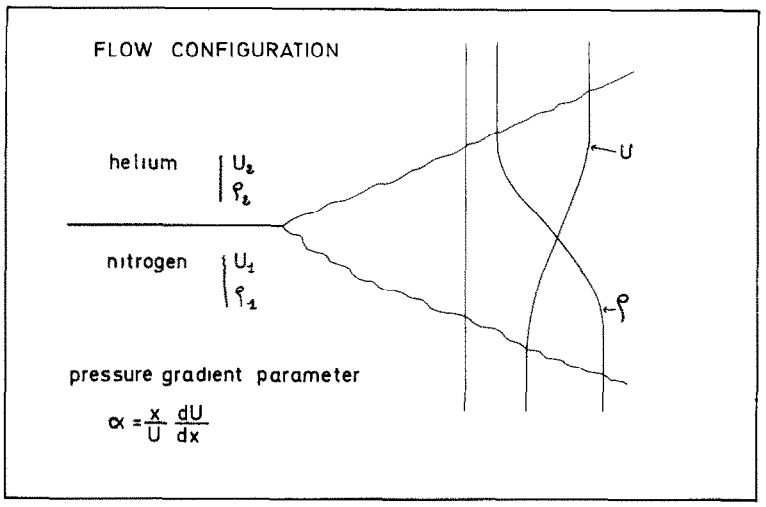

FIG. 1. Flow configuration.

The pressure gradient parameter α is defined as

$$\alpha = \frac{x}{u}\frac{\mathrm{d}u}{\mathrm{d}x}, \tag{2}$$

where u is the undisturbed velocity on either boundary of the shear layer. The measurements in [1] were performed for two cases: zero pressure gradient ($\alpha = 0$) and positive pressure gradient ($\alpha = -0.18$). It can be shown [1] that a self-similar flow with pressure gradient is possible only if the parameter α is constant. This condition cannot be applied to the region of the shear layer close to the physical (or virtual) origin, because $\alpha \neq 0$ and constant would imply that the pressure gradient goes to infinity as x approaches the origin. To remove this unnecessary and unphysical complication for the calculations, the pressure gradient in the initial region (*ca* 2.5 cm) was described by a polynomial giving zero pressure gradient at the origin and matching the value and the derivative of $\alpha = \text{const.}$ at the downstream end.

For the calculation the prescription of the upstream boundary values for all quantities determined from parabolic differential equations is necessary. The initial velocity profile consists of constant free

turbulent shear layer involving two gases with highly different densities. More recently, measurements in a methane–air free jet concerning the concentration field were reported [6]. From these available data the results of Rebollo [1] provided the best test case for the present study.

3. TURBULENCE MODEL

The turbulent shear flow described in the previous chapter exhibits large density variations due to the highly different densities at the lower and upper boundary. Therefore, it is appropriate to use density-weighted (Favre [7]) statistics for the description of the turbulent flow field. Dependent variables $\phi(\mathbf{x}, t)$, except density ρ and pressure p, are split into

$$\phi(\mathbf{x}, t) = \tilde{\phi}(\mathbf{x}, t) + \phi''(\mathbf{x}, t), \tag{3}$$

where the Favre-mean $\tilde{\phi}$ is defined as

$$\tilde{\phi}(\mathbf{x}, t) = \overline{\rho\phi}/\bar{\rho}, \tag{4}$$

and the unweighted mean is denoted by $\bar{\ }$. Averaging of the mass conservation equation leads to the closed equation

$$\frac{\partial \bar{\rho}}{\partial t} + \frac{\partial}{\partial x_\alpha}\bar{\rho}\tilde{v}_\alpha = 0. \tag{5}$$

The averaged momentum equations are

$$\frac{\partial}{\partial t}\bar{\rho}\tilde{v}_\alpha + \frac{\partial}{\partial x_\beta}\bar{\rho}\tilde{v}_\alpha\tilde{v}_\beta = -\frac{\partial\bar{p}}{\partial x_\alpha} - \frac{\partial}{\partial x_\beta}\bar{\rho}\widetilde{v_\alpha''v_\beta''} + \frac{\partial\overline{f_{\alpha\beta}}}{\partial x_\beta}, \quad (6)$$

where

$$\overline{f_{\alpha\beta}} = \mu\overline{\left(\frac{\partial v_\alpha}{\partial x_\beta} + \frac{\partial v_\beta}{\partial x_\alpha}\right)} - \frac{2}{3}\delta_{\alpha\beta}\mu\overline{D}, \quad (7)$$

and

$$D \equiv \frac{\partial v_\gamma}{\partial x_\gamma}.$$

The density-weighted kinetic energy of turbulence $\tilde{k} \equiv \frac{1}{2}\widetilde{v_\alpha''v_\beta''}$ satisfies (see [7])

$$\bar{\rho}\frac{\partial\tilde{k}}{\partial t} + \bar{\rho}\tilde{v}_\alpha\frac{\partial\tilde{k}}{\partial x_\alpha} = -\frac{\partial}{\partial x_\alpha}\left[\bar{\rho}\overline{v_\alpha''k''} + \overline{v_\alpha''p'} - \overline{v_\beta''f_{\beta\alpha}}\right] + \overline{p'D''} - \bar{\rho}\tilde{\varepsilon} - \bar{\rho}\widetilde{v_\alpha''v_\beta''}\frac{\partial\tilde{v}_\alpha}{\partial x_\beta} - \overline{v_\alpha''}\frac{\partial\bar{p}}{\partial x_\alpha}, \quad (8)$$

where the dissipation rate $\tilde{\varepsilon}$ satisfies a very complicated transport equation which will not be reproduced here.

The shear flow considered here can be treated as isothermal, thus reducing the energy equation to T = const. and eliminating temperature correlations. Composition and mixedness can be described either by partial densities and their second order moments or concentrations and their correlations. Introducing mass concentration c_i as

$$c_i = \frac{\rho_i}{\rho}; \qquad i = 1(1)N, \quad (9)$$

where N is the number of components in the mixture, it is easy to verify that

$$\widetilde{c_i} = \frac{\overline{\rho_i}}{\bar{\rho}}, \quad (10)$$

but

$$\overline{c_i} = \overline{\left(\frac{\rho_i}{\rho}\right)} \neq \widetilde{c_i}.$$

Therefore, it is not possible to express c_i in terms of first and second order unweighted moments and vice versa. Consequently, the choice of statistics for c_i must be made with respect to possible extensions of the model. For the treatment of chemical reactions with Borghi's approach [8] based on second order moments the description using partial densities is advantageous [9] and therefore chosen here. The equation for c_i follows as:

$$\frac{\partial}{\partial t}\bar{\rho}\widetilde{c_i} + \frac{\partial}{\partial x_\alpha}\bar{\rho}\tilde{v}_\alpha\widetilde{c_i} = \frac{\partial}{\partial x_\alpha}\left(-\bar{\rho}\widetilde{v_\alpha''c_i''} + \bar{\rho}\mathscr{D}_i\frac{\partial\widetilde{c_i}}{\partial x_\alpha} + \mathscr{D}_i\overline{\rho\frac{\partial c_i''}{\partial x_\alpha}}\right), \quad (11)$$

where $\mathscr{D}_i$ is the molecular diffusion coefficient according to the simplest approximation for multicomponent molecular diffusion as a Fick's law-type expression. The molecular term in equation (11) is in turbulent flows for sufficiently high Reynolds number negligible compared with turbulent diffusion except in the close vicinity of fixed walls, thus rendering the assumptions regarding $\mathscr{D}_i$ unimportant. For the description of mixedness of the shear flow the knowledge of the correlations,

$$\overline{Q_{ij}} \equiv \overline{\rho_i'\rho_j'}, \quad (12)$$

is essential. The Q_{ij} satisfy the following transport equation:

$$\frac{\partial\overline{Q_{ij}}}{\partial t} + \tilde{v}_\alpha\frac{\partial\overline{Q_{ij}}}{\partial x_\alpha} = -\frac{\partial}{\partial x_\alpha}\overline{v_\alpha''Q_{ij}} - D\overline{Q_{ij}} - \bar{\rho}\widetilde{c_i}\overline{\rho_j'D''} - \bar{\rho}\widetilde{c_j}\overline{\rho_i'D''} - \overline{v_\alpha''\rho_j'}\frac{\partial}{\partial x_\alpha}\bar{\rho}\widetilde{c_i} - \overline{v_\alpha''c_i'}\frac{\partial}{\partial x_\alpha}\bar{\rho}\widetilde{c_j} - \overline{\rho_j'\frac{\partial J_{i\alpha}}{\partial x_\alpha}} - \overline{\rho_i'\frac{\partial J_{j\alpha}}{\partial x_\alpha}}, \quad (13)$$

where the diffusive mass flux $J_{i\alpha}$ is defined as

$$J_{i\alpha} \equiv -\rho\mathscr{D}_i\frac{\partial c_i}{\partial x_\alpha}. \quad (14)$$

For a mixture of ideal gases, the averaged thermal equation of state is

$$\bar{p} = \bar{\rho}\overline{T}\Sigma R_i\tilde{c}_i\left(1 + \frac{\overline{\rho_i'T'}}{\bar{\rho}\overline{T}}\right). \quad (15)$$

For isothermal flows (15) reduces to

$$\bar{p} = \bar{\rho}\overline{T}\Sigma R_i\tilde{c}_i. \quad (16)$$

The system of equations considered so far contains various unknown correlations for which closed expressions must be given.

Closure assumptions

For simple shear flows with a dominant mean velocity component (parabolic in the mean) the concept of eddy transport coefficients is a satisfactory modelling assumption [4] for the prediction of first order moments. For flows with variable density several extensions of this concept can be stated, which are in general not equivalent. The following form will be employed here for the density-weighted Reynolds stress:

$$-\bar{\rho}\widetilde{v_\alpha''v_\beta''} \cong \mu_t\left(\frac{\partial\tilde{v}_\alpha}{\partial x_\beta} + \frac{\partial\tilde{v}_\beta}{\partial x_\alpha}\right) - \tfrac{2}{3}\delta_{\alpha\beta}(\mu_t\tilde{D} + \bar{\rho}\tilde{k}), \quad (17)$$

and for the turbulent flux of $\phi(\mathbf{x},t)$, the concept of turbulent Prandtl/Schmidt numbers σ_ϕ is invoked ($\phi \neq \rho$ and $\phi \neq p$):

$$-\bar{\rho}\widetilde{v_\alpha''\phi''} \cong \frac{\mu_t}{\sigma_\phi}\frac{\partial\tilde{\phi}}{\partial x_\alpha}, \quad (18)$$

where $\sigma_\phi = O(1)$ and constant. The turbulent (eddy)

viscosity μ_t is calculated from [10]

$$\mu_t = c_D \bar{\rho} \frac{\tilde{k}^2}{\tilde{\varepsilon}}, \tag{19}$$

where $\tilde{k} = \frac{1}{2}\widetilde{v_\alpha'' v_\beta''}$ is the turbulent kinetic energy and $\tilde{\varepsilon}$ the rate of dissipation of $\tilde{k}$.

Correlations of the form $\overline{\phi \cdot \psi}$, where ϕ and ψ are determined by different parts of the corresponding spectra (i.e., low and high wave number range), are modelled assuming statistical independence [5]:

$$\overline{\phi\psi} \cong \bar{\phi} \cdot \bar{\chi}. \tag{20}$$

For order of magnitude estimates the Schwarz-inequality is used together with further experimental evidence if available or results of computer optimization concerning cross-correlations. Furthermore correlations with the fluctuating pressure are neglected.

The system of modelled equations

The application of the modelling assumption (17) to the Reynolds stress term in the momentum equation for the dominant velocity component $\tilde{u}$ in a steady plane flow yields

$$\bar{\rho}\tilde{u}\frac{\partial \tilde{u}}{\partial x} + \bar{\rho}\tilde{v}\frac{\partial \tilde{u}}{\partial y} = -\frac{\partial \bar{p}}{\partial x} + \frac{\partial}{\partial y}\left(\mu_t \frac{\partial \tilde{u}}{\partial y}\right), \tag{21}$$

where the laminar stress term is neglected. The calculation of the eddy viscosity is based on the turbulent kinetic energy $\tilde{k}$ and its dissipation rate $\tilde{\varepsilon}$. Neglecting the correlation of pressure and velocity divergence and the diffusion of $\tilde{k}$ due to viscosity and pressure fluctuations in (8), the following modelled equation for $\tilde{k}$ is obtained using the modelling assumptions discussed above:

$$\bar{\rho}\tilde{u}\frac{\partial \tilde{k}}{\partial x} + \bar{\rho}\tilde{v}\frac{\partial \tilde{k}}{\partial y} = \frac{\partial}{\partial y}\left(\frac{\mu_t}{\sigma_k}\frac{\partial \tilde{k}}{\partial y}\right) + \mu_t\left(\frac{\partial \tilde{u}}{\partial y}\right)^2 - \bar{\rho}\tilde{\varepsilon} - c_p \frac{1}{\bar{\rho}}\sqrt{\overline{\rho'^2}\tilde{k}}\frac{\partial \bar{p}}{\partial x}. \tag{22}$$

The complicated structure of the exact nonclosed transport equation for the dissipation rate does not allow detailed modelling. Crude model assumptions [11] lead to

$$\bar{\rho}\tilde{u}\frac{\partial \tilde{\varepsilon}}{\partial x} + \bar{\rho}\tilde{v}\frac{\partial \tilde{\varepsilon}}{\partial y} = \frac{\partial}{\partial y}\left(\frac{\mu_t}{\sigma_\varepsilon}\frac{\partial \tilde{\varepsilon}}{\partial y}\right) + c_{\varepsilon_1}\mu_t\frac{\tilde{\varepsilon}}{\tilde{k}}\left(\frac{\partial \tilde{u}}{\partial y}\right)^2 - c_{\varepsilon_2}\bar{\rho}\frac{\tilde{\varepsilon}^2}{\tilde{k}} - c_{\varepsilon_3}\nu\frac{\partial^2}{\partial y^2}\left(\frac{1}{\bar{\rho}}\sqrt{\overline{\rho'^2}\tilde{k}}\right)\frac{\partial \bar{p}}{\partial x}, \tag{23}$$

which is analogous to the equation for the incompressible case [4]. Note that the term accounting for the pressure gradient in (22) and (23) vanishes for incompressible fluids as it must. For the mass transport equation (11), the modelling assumptions lead to

$$\bar{\rho}\tilde{u}\frac{\partial \widetilde{c_i}}{\partial x} + \bar{\rho}\tilde{v}\frac{\partial \widetilde{c_i}}{\partial y} = \frac{\partial}{\partial y}\left(\frac{\mu_t}{\sigma_i}\frac{\partial \widetilde{c_i}}{\partial y}\right), \tag{24}$$

where the laminar diffusive term and the density concentration derivative correlation have been neglected because both are one order of magnitude smaller than the leading term for high turbulent Reynolds numbers. The modelled equation for the density correlation $\overline{Q_{ij}}$ is given as

$$\bar{\rho}\tilde{u}\frac{\partial \bar{Q}_{ij}}{\partial x} + \bar{\rho}\tilde{v}\frac{\partial \bar{Q}_{ij}}{\partial y} = \bar{\rho}\frac{\partial}{\partial y}\left(\frac{\nu_t}{\sigma_Q}\frac{\partial \bar{Q}_{ij}}{\partial y}\right) - \bar{\rho}\tilde{D}\bar{Q}_{ij} + 2\frac{\mu_t}{\sigma_i}\frac{\partial}{\partial y}\bar{\rho}\widetilde{c_i}\frac{\partial}{\partial y}\bar{\rho}\widetilde{c_j} - c_{Q_1}\bar{\rho}\frac{\tilde{\varepsilon}}{\tilde{k}}\bar{Q}_{ij} - c_{Q_2}\bar{\rho}\frac{\tilde{\varepsilon}}{\tilde{k}}(\widetilde{c_i}\overline{\rho'\rho_j'} + \widetilde{c_j}\overline{\rho'\rho_i'}). \tag{25}$$

From the definition of the mass fraction c_i follow the local relations:

$$\overline{\rho'^2} = \sum_i \sum_j \bar{Q}_{ij} \tag{26}$$

and

$$\overline{\rho'\rho_i'} = \sum_j \bar{Q}_{ij}. \tag{27}$$

The mean density $\bar{\rho}$ is obtained from (16) for isothermal flows without difficulty.

Realizability conditions

Modelled transport equations for statistical moments do not ensure that their solutions will satisfy all mathematical constraints for moments unless the closure assumptions incorporate the constraints. The density correlations $\bar{Q}_{ij}$ in particular must satisfy the following inequalities, if the instantaneous density ρ has the upper bound ρ_0. A binary mixture with components A and B is considered. For this case and negligible pressure fluctuations and constant temperature it can be shown (using the equation of state) that the instantaneous density ρ is bounded by the maximal density on the boundary of the flow field. This upper bound ρ_0 for $\rho(x,t)$ is the density of the mixture consisting of the fluid with the larger molecular mass only. Then the autocorrelations are bounded by

$$0 \leqslant \bar{Q}_{AA} \leqslant \rho_0 \bar{\rho} c_A\left(1 - \frac{\bar{\rho}}{\rho_0}\widetilde{c_A}\right) \tag{28}$$

and

$$0 \leqslant \bar{Q}_{BB} \leqslant \rho_0 \bar{\rho} c_B\left(1 - \frac{\bar{\rho}}{\rho_0}\widetilde{c_B}\right). \tag{29}$$

The cross correlation is bounded by

$$-\bar{\rho}^2\widetilde{c_A}\widetilde{c_B} \leqslant \bar{Q}_{AB} \leqslant \bar{\rho}\rho_0 \cdot \times \min\left[\widetilde{c_B}\left(1 - \frac{\bar{\rho}}{\rho_0}\widetilde{c_A}\right), \widetilde{c_A}\left(1 - \frac{\bar{\rho}}{\rho_0}\widetilde{c_B}\right)\right]. \tag{30}$$

The mean mass functions obviously satisfy

$$0 \leqslant \widetilde{c_i} \leqslant 1. \tag{31}$$

In order to enforce these conditions, the solution of the modelled transport equations was checked at every step and clipped if necessary.

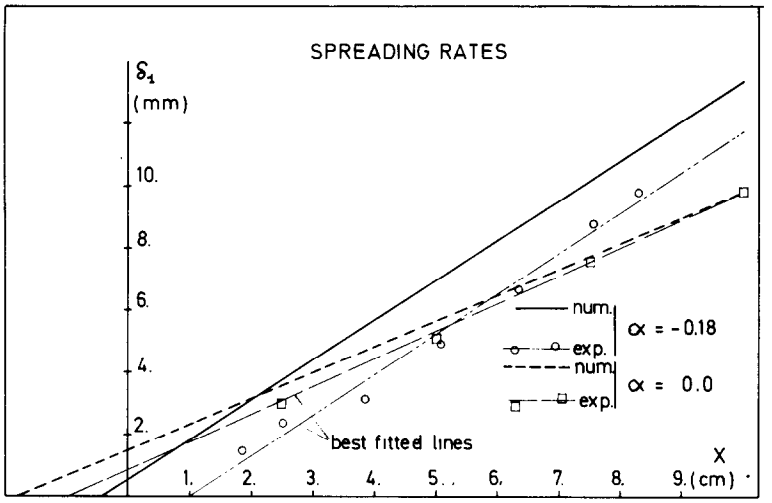

FIG. 2. Spreading rates of plane shear layer for zero pressure gradient ($\alpha = 0$) and positive pressure gradient ($\alpha = -0.18$), measurements from [1].

4. RESULTS

All the calculations were made with the boundary conditions described in Section 2 and the values of the constants given in Table 1. An important parameter describing the global development of the mixing layer is the spreading rate. Defining

Table 1. Constants of turbulence model

σ_k	σ_ε	σ_A	σ	c_{ε_1}	c_{ε_2}	c_{ε_3}	c_p
1.0	1.3	0.26	0.26	1.45	2.0	0.4	0.4

N_2–N_2		H_e–N_2		H_e–H_e	
C_{Q_1}	C_{Q_2}	C_{Q_1}	C_{Q_2}	C_{Q_1}	C_{Q_3}
5.0	0.6	3.0	0.6	2.0	0.5

$\Delta u = u_2 - u_1$ the characteristic thickness δ_1 with respect to the velocity profile is taken as the distance between the points with $u_1 + 0.2\Delta u$ and $u_1 + 0.8\Delta u$ in accordance with [11]. The following values were obtained for the spreading rate $d\delta_1/dx$ (see Fig. 2):

$\alpha = 0$ (zero pressure gradient):

$$\frac{d\delta_1}{dx} = \begin{cases} 0.1 & \text{experiment [1]} \\ 0.085 & \text{calculation} \end{cases}$$

$\alpha = -0.18$ (positive pressure gradient):

$$\frac{d\delta_1}{dx} = \begin{cases} 0.128 & \text{experiment [1]} \\ 0.130 & \text{calculation.} \end{cases}$$

The comparison of the thickness δ_1 with the experimental values in Fig. 2 shows good agreement for $\alpha = 0$, but for $\alpha = -0.18$ the calculated curve is shifted above the experimental values with the spreading rate in good agreement. This discrepancy is due to the lack of information about the initial velocity profile and the pressure gradient distribution in the initial region ($0 \leqslant x \leqslant 2.5$ cm) which was

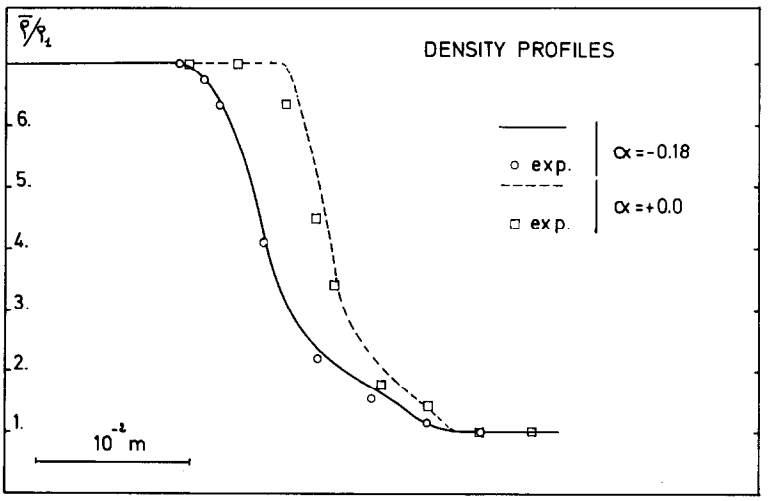

FIG. 3. Mean density profiles for $\alpha = 0$ and $\alpha = -0.18$ at $x = 5.08$ cm measurements from [1].

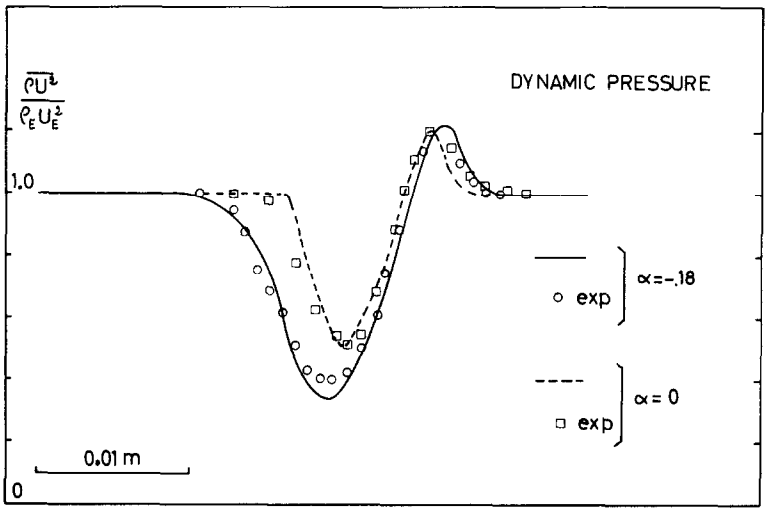

FIG. 4. Dynamic pressure for $\alpha = 0$ and $\alpha = -0.18$ at $x = 5.08$ cm, measurements from [1].

interpolated (see Section 2). The thickness of the initial velocity profile was estimated from the length of the splitter plate and the Reynolds number based on free stream velocity and kept constant for both cases.

The agreement between measured and calculated mean values is good as shown in Figs. 3 and 4. The mean dynamic pressure from the experiments is close to $\overline{\rho u^2}$ and this quantity is related by

$$\overline{\rho u^2} = \bar{\rho}\tilde{u}^2 + \bar{\rho}\widetilde{u''^2}, \tag{32}$$

to the Favre-averaged variables. For $\widetilde{u''^2} \cong 2/3k$, the second term is below 2% of the first and the correction becomes negligible. The dynamic pressure in Fig. 4 has two characteristic features: the undershoot due to the wake of the splitter plate, and an overshoot which is a consequence of the variable density. The overshoot is of particular interest because it does not appear in constant density flows. It appears on the low density–high velocity side of the shear later. Within the framework of the calculation model suggested in this paper, the overshoot can only appear if the turbulent Schmidt number σ_A is significantly smaller than unity (between 0.2 and 0.3), which is in agreement with the similarity analysis in [1], but not with the values ($\sigma_f \cong 0.6$ [12]) for the turbulent Schmidt number of the mixture fraction used in calculations for turbulent reacting flows with similar levels of density fluctuations. To study the influence of the Schmidt number σ_A on the development of the overshoot in the shear layer with and without pressure gradient several runs with different σ_A were made. The results plotted in Fig. 5 show for the case $\alpha = 0$ (zero pressure gradient) a simple relation between σ_A and the amount of overshoot, whereas for the case with positive pressure gradient ($\alpha = -0.18$) the relation is more complex. This is due to the direct influence of the density fluctuations via the pressure gradient on the development of k and ε in (22) and (23).

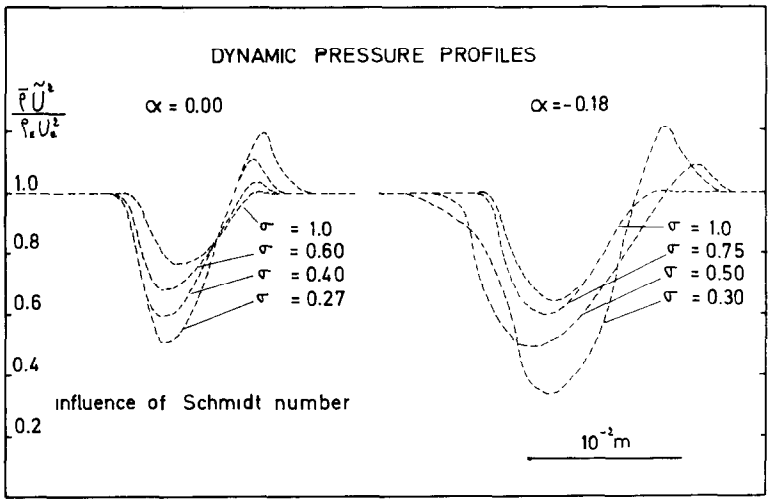

FIG. 5. Influence of turbulent Schmidt number σ_A on dynamic pressure for $\alpha = 0$ and $\alpha = -0.18$.

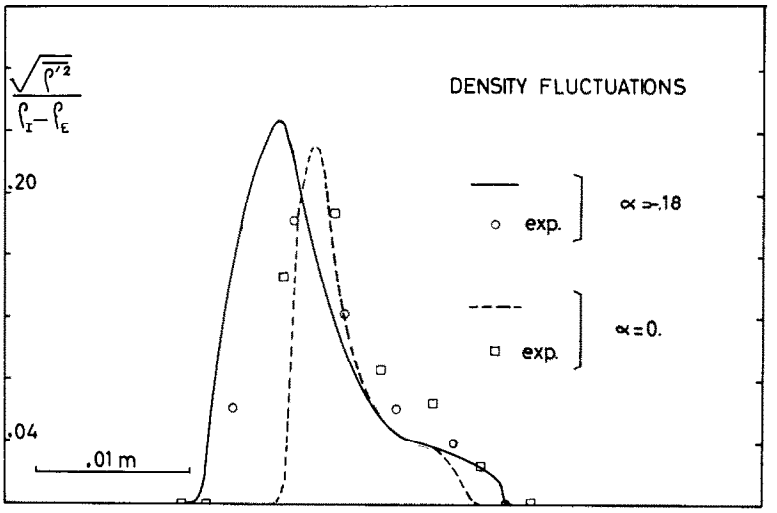

FIG. 6. Intensity of density fluctuations for $\alpha = 0$ and $\alpha = -0.18$ at $x = 5.08$ cm, measurements from [1].

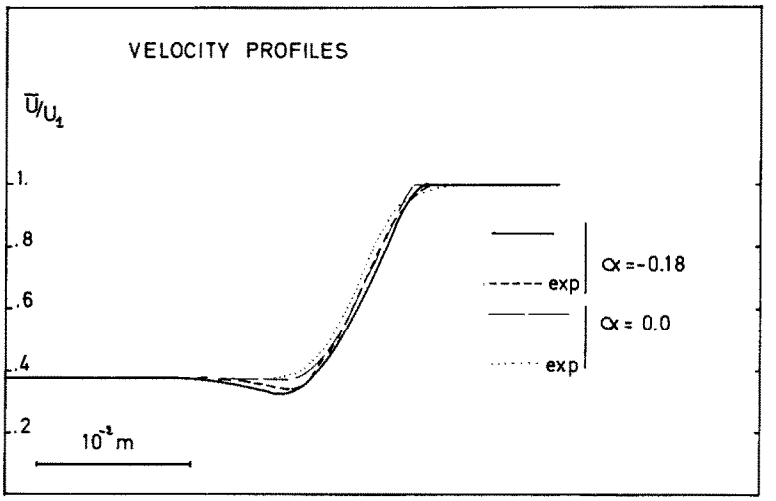

FIG. 7. Mean velocity for $\alpha = 0.0$ and $\alpha = -0.18$ at $x = 5.08$ cm, experimental values [1] calculated from mean density and dynamic pressure.

The mean velocity profiles in Fig. 7 are compared with profiles calculated from the measured values for the mean density and the mean dynamic pressure. The solution of (21) is the Favre-mean velocity whereas the velocity calculated from the experimental results is something between the weighted and unweighted average. But the difference between the two velocities can be expected to be small, because the error in the dynamic pressure is small and the comparison is still possible. Taking this fact into account the agreement between calculated and (indirectly) measured mean velocity is acceptable.

The density fluctuations variance in Fig. 6 show agreement between calculation and experiment in level and form of the profile. At the location of the overshoot of the dynamic pressure the variance profile exhibits a characteristic step-like form indicating relatively strong fluctuations, which are present in the calculated profile but still too small.

For the comparison between calculated and measured shear stress in Fig. 8, the same reservation as in the case of the mean velocity has to be made, but with possibly larger errors. The calculated values are noticably smaller than the experimental ones but the shapes of the profiles agree quite well. For the flow with positive pressure gradients, the calculated shear stress shows a slight undershoot on both sides which is not recognizable in the experiments on the right end of the profiles. It is a consequence of a slight over- and undershoot in the mean velocity profiles (Fig. 7), but the difference on the right side (high velocity–low density side) is probably due to the underprediction of the level of the density fluctuations in this part, which in turn changes the turbulent viscosity via the pressure gradient term in the k and ε equations.

5. CONCLUSIONS

A free turbulent shear flow with strong density fluctuations due to the mixing of two different gases was calculated using a turbulence model based on the k–ε system suggested by Jones and Launder [10].

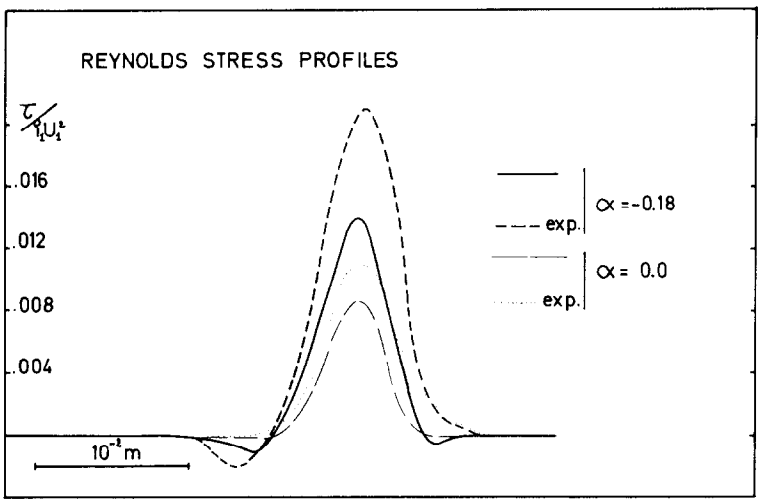

FIG. 8. Turbulent shear stress for $\alpha = 0.0$ and $\alpha = -0.18$ at $x = 5.08$ cm, experimental values [1] calculated from mean density and dynamic pressure.

The transport equations for the correlations of partial density fluctuations were included in the model to obtain good agreement of the variance of the total density fluctuations with the values measured by Rebollo [1]. The results of the calculations lead to the following conclusions:

(1) The turbulent Schmidt number σ_A for the gradient flux model describing the turbulent transport of mass in crossflow direction must be small ($\sigma_A \cong 0.26$) compared to unity in order to produce the overshoot of the dynamic pressure found experimentally. For the zero pressure gradient flow σ_A determines the turbulent diffusion of the mean concentration c_A which in turn determines the mean density (16) and influences the turbulent viscosity via (19). But for nonzero pressure gradient an additional effect appears in the k and ε equations (22) and (23) as pressure gradient source/sink term is modelled as being proportional to the density fluctuation intensity $[\overline{\rho'^2}]^{1/2}$. The intensity $[\overline{\rho'^2}]^{1/2}$ in turn is determined by $\bar{Q}_{ij}$, which contain σ_A in the corresponding production terms. This leads to the more complex dependence of the dynamic pressure overshoot for $dp/dx > 0$ compared with $dp/dx = 0$ shown in Fig. 5.

The Schmidt number σ_A was kept constant with respect to coordinates in the calculations which does not correspond to the profile for σ_A found by [1], where σ_A increases as the highly intermittent boundary parts of the shear layer are approached. This tendency is in contrast to the Prandtl number profile found by Chevray and Tutu [13] for the transport of heat in a free jet. The concept of turbulent Prandtl/Schmidt numbers applies well in the core region (large gradients) of the turbulent shear layer, but not so well in the highly intermittent (small gradient) boundary regions.

(2) The mean density and the $\overline{\rho'^2}$ profiles show a characteristic hump on the high velocity–low density side of the shear layer roughly in the region of the dynamic pressure overshoot. This leads to the conclusion that the turbulence mixes mass more efficiently in this region than momentum. This is reflected in the small value of σ_A.

REFERENCES

1. M. R. Rebollo, Analytical and experimental investigation of a turbulent mixing layer of different gases in a pressure gradient, Ph.D. Thesis, California Institute of Technology (1973).
2. W. Rodi, A review of experimental data of uniform density free turbulent boundary layers, in *Studies in Convection*, edited by B. E. Launder. Vol. 1, pp. 79–165. Academic Press, New York (1975).
3. Free turbulent shear flows; Conference Proceedings, Vol. 1. NASA SP 321 (1972).
4. Turbulent shear flow; Symposium Proceedings, Vol. 1. The Pennsylvania State University, U.S.A. (1977).
5. G. L. Brown and A. Roshko, On density effects and large structure in turbulent mixing layers, *J. Fluid Mech.* **64**, 775 (1974).
6. A. D. Birch, D. R. Brown, M. G. Dodson and J. R. Thomas, The turbulent concentration field of a methane jet, *J. Fluid Mech.* **88**, 431 (1978).
7. A. Favre, Equations des gaz turbulents compressibles, *J. Méc.* **4**, 361, 391 (1965).
8. R. Borghi, Chemical reactions calculations in turbulent flows. AGARD CP 164, pp. II 1–4 (1976).
9. J. Janicka and W. Kollmann, Ein Rechenmodell für reagierende turbulente Scherströmungen im chemischen Nichtgleichgewicht, *Wärme- und Stoffübertragung* **11**, 157 (1978).
10. W. P. Jones and B. E. Launder, The prediction of laminarization with a two equation model of turbulence. *Int. J. Heat Mass Transfer* **15**, 301 (1972).
11. W. Kollmann, Analysis of the turbulent mixing process in downstream mixing gasdynamic lasers, VKI IN 56 (1977).
12. S. Elgobashi, Studies in the prediction of turbulent diffusion flames, in *Studies in Convection*, edited by B. E. Launder. Vol. 2, pp. 141–189. Academic Press, New York (1977).
13. R. Chevray and N. K. Tutu, Intermittency and preferential transport of heat in a round jet, *J. Fluid Mech.* **88**, 133 (1978).

CALCUL DES ECOULEMENTS TURBULENTS A CISAILLEMENT AVEC DE GRANDES FLUCTUATIONS DE DENSITE

Résumé—On étudie le mélange turbulent de deux gaz de masses moléculaires très différentes dans une couche de cisaillement plane. Un modèle de calcul incorporant des équations de transport modélisées pour les fluctuations de densité est développé et les résultats numériques sont comparés aux mesures avec lesquelles ils sont en bon accord.

DIE BERECHNUNG VON FREIEN, TURBULENTEN SCHERSTRÖMUNGEN MIT STARKEN DICHTESCHWANKUNGEN

Zusammenfassung—Der turbulente Mischungsprozess zweier Gase von stark unterschiedlicher Molmasse in einer ebenen Scherströmung wird untersucht. Ein Rechenmodell, das modellierte Transportgleichungen für die Korrelationen der Partialdichten enthält, wird entwickelt. Die numerischen Resultate werden mit Messwerten verglichen und zeigen gute Übereinstimmung.

РАСЧЁТ ТУРБУЛЕНТНЫХ СДВИГОВЫХ СВОБОДНЫХ ТЕЧЕНИЙ ПРИ ИНТЕНСИВНЫХ ПУЛЬСАЦИЯХ ПЛОТНОСТИ

Аннотация — Рассматривается турбулентное смешение двух газов с сильно отличающимися молекулярными массами в плоском слое смешения. Разработана модель расчёта, содержащая модельные уравнения переноса пульсаций плотности различных компонент газа; результаты расчётов сопоставлены с данными измерений. Получено хорошее совпадение результатов.